RESEARCH ARTICLE

Electrochemical sensor based on epoxy-functionalized BEA nanozeolite and graphene oxide modified glassy carbon electrode for bisphenol E determination

Alex H. Miller[1,2,3] · Huong Thi-Thanh Nguyen[1] · José G. Nery[2] · Alistair J. Fielding[1]

Abstract

An epoxy-functionalized beta type nanozeolite (BEA)/graphene oxide nanocomposite modified glassy carbon electrode (GCE/BEA/APTMS/GA/GO/NF) has been created for the differential pulse voltammetric determination of bisphenol E (BPE). The modified electrode presented an enhanced current response in comparison with bare GCE. A linear dependence of anodic peak current (I_p) and scan rate (ν) was observed, which showed that the electrochemical process was adsorption-controlled. Differential pulse voltammetry (DPV) was employed and optimized for the sensitive determination of BPE. Under the optimized conditions, the anodic peak current was linearly proportional to BPE concentration in the range between 0.07 and 4.81 µM, with a correlation coefficient of 0.995 and limit of detection 0.056 µM (S/N = 3). The electrode showed good repeatability and storage stability, and a low response to interfering compounds. Comparison was made to the determination of bisphenol A. To confirm the electrode analytical performance, recovery tests were performed, and deviations lower than 10% were found. The BEA zeolite-GO nanocomposite proved to be a promising sensing platform for bisphenol determination.

Graphical abstract
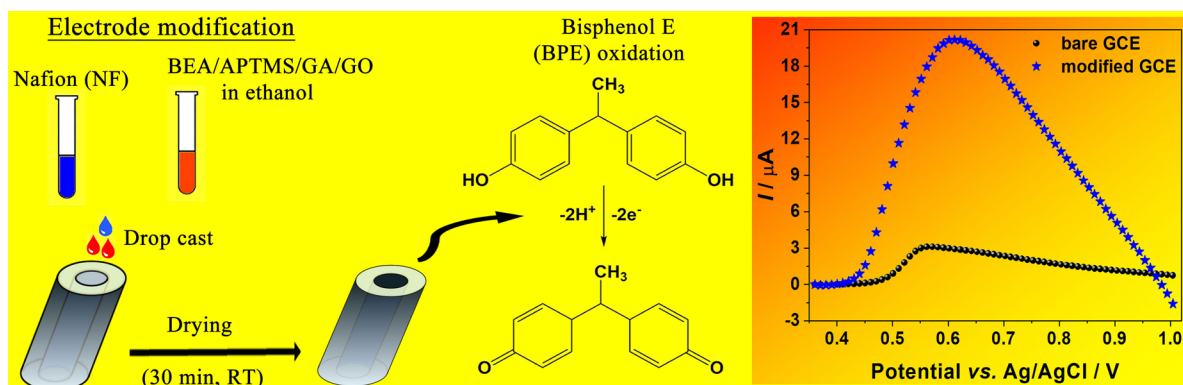
Keywords BEA nanozeolite · Graphene oxide · Bisphenol E · Bisphenol A · Electrochemistry

1 Introduction

Bisphenols (BPs) are a known group of endocrine disrupting compounds with adverse effects on human health and the environment [1]. Bisphenol A (BPA), 2, 2-bis (4-hydroxy-phenyl) propane, is the most used among BPs with a wide range of applications, such as polycarbonate plastics manufacturing, with potent endocrine-disrupting activity.

✉ Alistair J. Fielding
a.j.fielding@ljmu.ac.uk

Extended author information available on the last page of the article

Bisphenol E (BPE), 1,1-bis(4-hydroxyphenyl) ethane, which has a structure very similar to BPA (Fig. 1) is another important industrial chemical used as monomer for the production of polycarbonate plastics and epoxy resins [2]. BPE has been reported to have similar acute toxicity and estrogenic activity to that of BPA [, , , , 2–6].

Conventional chromatography, such as liquid chromatography (LC) or gas chromatography (GC), sometimes combined with mass-spectroscopy (MS); LC–MS and GC–MS; and/or UV–Vis spectroscopy are sensitive and selective analytical procedures for the routine determination of BPs. Disposable or simple manufactured tools have been widely used for environmental analysis in the last couple of years, in which electrochemical sensors or biosensors stand as good options due to their wide applicability and feasibility [, , 1, 7, 8]. Advances in the area of nanostructured materials, have made possible the design of a series of different electrochemical sensors, where nanocomposites are used to decorate conventional glassy carbon electrodes (GCE) or screen printed electrodes (SPE) with reported increased sensitivity and/or selectivity for the determination of BPs [, , , , , , , , , , 9–19]. Graphene oxide (GO) nanocomposites or hybrids with other materials [, , , , , , 20–26] are also examples of nanomaterials used for this purpose. Surfactants, dendrimers, ionic liquids, among others, are additional materials used for the preparation of electrochemical sensors for BPs determination [, , , , 27–31].

Among many different materials, micro- and nano-sized zeolites have attracted extensive attention due to their multifunctional properties such as small sizes, biocompatibility, high surface area, and the possibility of modulation [32] of their hydrophilicity and hydrophobicity on electrode surfaces for applications of sensing [, , , 33–36] and biosensing [, , , , , , 37–43]. An electrochemical sensor for BPA quantification using ZrO_2 supported Nano-ZSM-5 nanocomposite with nanomolar sensitivity has been reported recently [44], and used for real sample analysis.

Although a wide range of different electrodes have been reported for BPA determination, few works have targeted BPE and/or studied its potential interference properties during electrochemical analytical methods used for BPs. Lu et al. [45] reported a Metal–Organic Framework (MOF)-based tyrosinase electrochemical sensor for a series of BPs, including BPE, with nanomolar sensitivity.
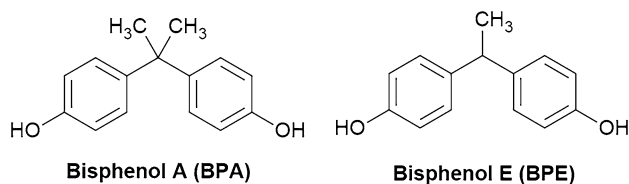
They indicated that the BPs molecular structure influenced electrode performance. Recently, Vaghela et al. [46] described the preparation of a electrochemical bioelectrode containing entrapped tyrosinase in an agarose-guar gum-graphene oxide composite cast on indium titanium oxide (ITO) glass plates. The mechanism of sensing involved enzymatic oxidation of bisphenols to corresponding o-bisphenols and subsequently their reduction on the designed bioelectrodes at a potential of 80 mV. The limit of detection found for BPE was 10 μM. To our knowledge, there are no reports of zeolitic nanocomposites applied to BPE electrochemical determination.

The creation of electrodes using zeolite in combination with graphene oxide (GO) has been reported [36]. GO is known for its high electronic conductivity, relatively inert electrochemistry, biocompatibility, wide potential range and low cost [47], and can act as a reinforcement for the assembling of oxides to form stable sensing platforms [48]. These properties in combination with zeolites has led to a great increase of the sensitivity [, , 36, 49, 50]. In a previous work, we reported the synthesis and characterization of nanozeolites, such as beta type zeolite (BEA), and its alkoxysilane functionalization with (3-aminopropyl) trimethoxysilane (APTMS), followed by cross-linking with glutaraldehyde (GA) [32]. Herein, we report the application of BEA/APTMS/GA and GO decorated GCE to bisphenol E determination. Unmodified and modified nanozeolite and GO suspensions were prepared in ethanol and used for GCE coating by a drop coating method. Nafion (NF) polymer was used to complete the coating and guarantee that modifiers did not leach from the electrode surface. The intensity of the oxidation peak of BPE was significantly increased when using GCE/BEA/APTMS/GA/GO/NF in comparison with bare GCE or other tested modified electrodes. This electrode was then selected for further investigation of its electrochemical properties and analytical performance.

2 Experimental

2.1 Reagents

Aluminum isopropoxide (98%), tetraethylammonium hydroxide solution (20%), Cab-O-sil® M-5, graphene oxide (15–20 sheets, 4–10% edge-oxidized), Nafion solution (5 wt%), ethanol (99.8%), inorganic salts, glutaraldehyde solution (25%), (3-aminopropyl)trimethoxysilane (APTMS, 97%), and anhydrous dichloromethane were purchased from Sigma-Aldrich. All chemicals were used without further purification.

Fig. 1 Bisphenols A and E structures

2.2 Instrumentation

The crystallographic structure and morphology of the synthetized nanozeolite were determined by X-ray diffraction (XRD) and scanning electron microscopy (SEM). The XRD analyses were performed with a MiniFlex II instrument (Rigaku, Tokyo, Japan) equipped with a rotating anode source with flat-plate Bragg–Brentano geometry and a graphite monochromator, operating at 40 kV and 40 mA, with Cu Kα radiation (wavelength = 1.5418 Å). The powder diffraction patterns were recorded in the 2θ range from 3° to 50°, with scanning at a goniometer rate of $2°$ min^{-1}. SEM images were recorded using a Magellan 400 L instrument (FEI Company), with deposition of a thin coating of gold onto the samples prior to the analyses. Surface alkoxysilane functionalization was measured using Fourier transform infrared (FT-IR). FT-IR spectra were acquired using a PerkinElmer Frontier FT-IR spectrometer equipped with an ATR accessory. The samples were scanned 64 times between 4000 and 400 cm^{-1}, at a resolution of 4 cm^{-1}.

All electrochemical apparatus, including electrodes, was purchased from Metrohm, Netherlands. The electrochemical process was performed using Autolab potentiostat/galvanostat equipment (PGSTAT 101), and data processed using NOVA 2.1.4 software. A three-electrode cell was employed using Ag/AgCl (3 M KCl) as reference electrode and a platinum wire as counter-electrode (all potentials hereafter presented follow this reference). A glassy carbon electrode (GCE) (3 mm diameter) was used as working electrode in its original form and after surface modification. Bare and modified electrode surfaces were characterized by SEM using an Inspect S50 microscope (FEI company), with deposition of a thin coating of gold onto the modified electrodes prior to the analyses.

2.3 The synthesis BEA type nano-sized zeolite

The beta nanozeolite (BEA) synthesis was adapted from the procedure described by Larlus et al. [51]. The synthesis gel was prepared by dissolving 0.56 g of aluminum isopropoxide in 37.0 g of tetraethylammonium hydroxide solution (TEAOH, 20%) under magnetic stirring for 1 h, followed by the addition of 6.05 g of Cab-o-sil. The precursor gel was stirred and aged overnight at room temperature. Afterward, the gel was transferred to steel autoclaves with 120 mL Teflon liners, and the syntheses performed under autogenous conditions for 5 days at 140 °C. The nanocrystals were cooled to room temperature, recovered by centrifugation 13,400×g (Hitachi Koki Himac CR22N High-Speed Refrigerated Centrifuge), washed with deionized water until reaching pH < 8, and dried at 80 °C for 12 h. The as synthesized material was then calcinated at 600 °C for 9 h to remove the organic templates. Calcinated material hereafter denoted BEA. See Figure S1 for XRD patterns and SEM images.

2.4 BEA and GO functionalization

The BEA was alkoxysilane surface functionalized as previous reported [32]. Initially, 1 g of BEA was suspended in a solution containing 30 mL of dichloromethane and 1 mL of APTMS, and the suspension stirred for 16 h at room temperature. The obtained material was then centrifuged (13,400×g) and washed several times with distilled water to remove the unreacted APTMS. The final precipitated was dried at 60 °C for 12 h, and denoted BEA/APTMS. Finally, the BEA/APTMS functionalized nanozeolite was cross-linked with glutaraldehyde (GA). The experiment was performed as follows: 1 g of BEA/APTMS nanozeolite was mixed with 20 mL of a 5% glutaraldehyde solution by magnetic stirring for 24 h at room temperature. The GA-functionalized nanozeolite was collected by centrifugation (13,400×g) and the solid product was washed three times with distilled water, dried at room temperature, and stored under vacuum in order to prevent oxidation. Cross-linked material denoted BEA/APTMS/GA (See Fig. S1 for FT-IR characterization). The GO functionalization with APTMS was adapted from Lin et al. [52]. 200 mg GO was dispersed into 50 mL toluene and sonicated for 30 min. Next, 1.3 mL of APTMS was added and the mixture refluxed under nitrogen atmosphere at 30 °C for 3 h and then at 100 °C for another 3 h. Following, the reaction product was filtered and washed thrice with toluene to remove the residual APTMS. The filtrate was dried in an over at 40 °C overnight, solid product denoted GO/APTMS. The GO/APTMS was then cross-linked with glutaraldehyde in the same fashion as the BEA/APTMS. Resulting material denoted GO/APTMS/GA (See Fig. S2 for FT-IR characterization).

2.5 The glassy carbon electrode modification

The GCE electrode was modified by the drop cast method. Initially, stock solutions (5 mg/mL) of BEA/APTMS/GA and GO were prepared in ethanol, followed by 30 min sonication for effective dispersion of the solid materials. The modifier BEA/APTMS/GA/GO solution was prepared by mixing the suspensions obtained in a 1:1 proportion BEA/APTMS/GA:GO immediately after sonication to minimize precipitation and concomitantly achieve reproducible preparations. A 1.5% Nafion (NF) solution was also prepared by diluting the 5% concentrated commercial solution in ultrapure water. Before modification, the GCE surface was polished using 0.3 μM alumina in a polishing pad, followed by sonication in ethanol and ultrapure water for 5 min each, respectively, for the elimination of polishing residues. The casting process consisted of dropping with use of a

micropipette two layers of 2 μL each of BEA/APTMS/GA/GO solution (sonicated for 1 min right before pipetting), 5 min wait for ethanol evaporation, followed by a final 2 μL layer of NF solution. The NF solvent evaporation was performed in open air and room temperature for 30 min. The obtained modified electrode is hereafter denominated GCE/BEA/APTMS/GA/GO/NF. Other GCE modifications using as modifiers NF, BEA/NF, BEA/APTMS/NF, BEA/APTMS/GA/NF, GO/NF, GO/APTMS, GO/APTMS/GA, GO/BEA/NF, and GO/BEA/APTMS/NF were performed following the same procedure.

2.6 Electrochemical tests

The electrochemical characterization of the sensor was made by use of cyclic voltammetry (CV) and differential pulse voltammetry (DPV). The CV voltammograms were recorded in a potential range from -0.3 to 1.0 V using a scan rate of 50 mVs^{-1}. The supporting electrolyte initially used was a 0.1 M sodium phosphate buffer solution, pH 5. A typical experiment was performed as follows: 20 mL of 50 μM BPE solution in phosphate buffer was poured into the voltammetric cell. Before measurements, nitrogen gas was purged into the solution for 5 min, and the atmosphere was kept under nitrogen flow throughout the measurements to avoid oxygen gas dissolution. The pH dependence was studied using Britton–Robinson buffer to reduce the influence of supporting electrolyte on current values, as it can cover a broad range of pH values. Prior to DPV measurements, the freshly made electrode was submitted to 20 CV's cycles in phosphate buffer, pH 5, to verify its stabilization (reproducible baselines). Following, 15 mL of various concentrations of analyte solutions were added into the cell. A pre-conditioning step before DPV measurement was performed, in which the solution was purged with nitrogen gas while under vigorous stirring at an applied potential of 0.5 V for 90 s. The DPV recording proceeded in static state with no further purging. The increment potential, pulse period, pulse amplitude, and pulse width were adjusted at 0.075 mV, 0.4 s, 0.05 V, and 0.075 s, respectively. All measurements were performed in triplicate for statistical mean.

2.6.1 Recovery tests

Tap water from Liverpool John Moores University was collect in a 200 mL glass container, filtered using 45 μm filters and stored at 4 °C for further analysis. Measurements were performed using DPV optimized parameters. Recovery tests carried out using the standard addition method with concentrations within the linear range obtained for the analytical calibration.

3 Results and discussion

3.1 BPE cyclic voltammetry at bare and modified GCE

The search for a more sensitive electrode consisted in comparative experiments using CV to study the oxidation of BPE at bare GCE and at a series of modified electrodes: BEA and BEA derivatives only; GO only; GO derivatives; and finally, the BEA and BEA derivatives mixtures with GO. Figure 2 shows the oxidative part of CVs curves arising from 50 μM BPE in 0.1 M phosphate buffer solution (pH 5) for some of the modified electrodes in comparison with bare GCE. To illustrate the analyte oxidation current despite background, the baselines (only buffer) were subtracted from the analyte's measurements and only the oxidative scan presented (see Supplementary Info, Fig. S3, to check the raw data full voltammograms). Oxidation peaks are noted in all curves, and the absence of reduction peaks (not shown) indicated that the process was irreversible (see Fig. S3). The results are similar to what is known for the analogous bisphenols BPA [, , 10, 53, 54], BPF [, 12, 13], and TBrBPA [, 55, 56].

Figure 2 highlights the results for the bare GCE in comparison with GCE covered with BEA/APTMS/GA/NF, GO/NF, GO/BEA/APTMS/GA/NF, and GO/APTMS/GA/NF. Lower anodic peak current intensity (I_p) was noted for modified BEA based electrode in absence of GO. However, GCE/GO/NF presented an increase of I_p, and the electrode GCE/BEA/APTMS/GA/GO/NF had a remarkable increase
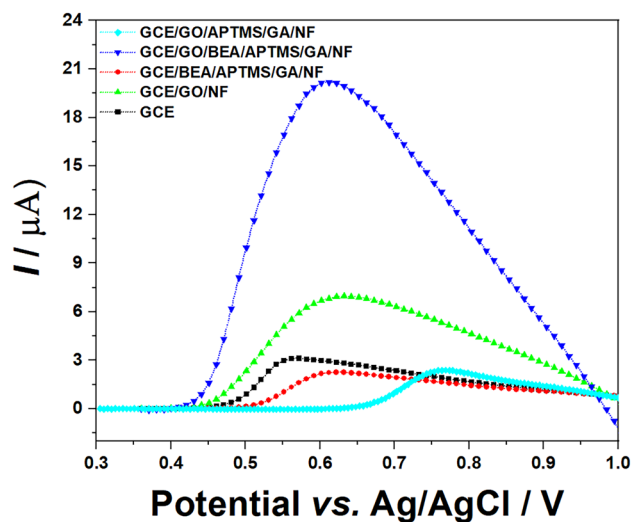
Fig. 2 The CV curves of 50 μM BPE solutions in 0.1 M phosphate buffer solution (pH 5) at bare or modified GCE electrodes (only oxidative scan shown). Scan rate: 50 mVs^{-1}, under N$_2$ atmosphere. Background was first recorded in the absence of analyte and subtracted from the respective voltammograms. (see Fig. S3 for the respective unsubtracted full voltammograms)

of around seven folds higher than the bare GCE. All components of the GCE/BEA/APTMS/GA/GO/NF electrode were tested separately, and none by itself gave a similar I_p to the BEA/APTMS/GA/GO/NF modified electrode. Intermediate electrodes of the constituent parts gave analogous or slightly higher I_p in comparison to the bare GCE electrode (Fig. S3). To evaluate whether the functional groups arising from APTMS and GA would lead to higher I_p in the absence of zeolite, the functionalization of GO with both reagents was carried out. Despite significant peak shift, the maximum current was not much different than that found for the bare electrode (Fig. 2), and significantly lower than unmodified GO, which indicated that the addition of APTMS and GA to GO had a negative influence on the electrode sensitivity. It is reasonable to attribute the increased current output to a coactive interaction between the coating components, which led to a more favorable BPE interaction with the electrode surface. Overall, Fig. 2 shows that the modified zeolite combined with GO was required for increased BPE electrooxidation.

Some reasonable understanding as to the causes of these observations can be made based on the chemistry of modified zeolites. It is clear that the nanozeolite functional surface groups have a crucial role on the sensor electrochemical performance, consistent with previous reports of very complex processes occurring where functional groups were included to improve the analyte interaction with the electrode and concomitantly the quantification [, , , , 19, 20, 22, 23, 57]. Based on our previous experience of zeolites functionalization [32], where alkoxysilane functionalization was performed, followed by glutaraldehyde cross-linking, zeolitic surface electrostatic changes were observed by zeta

potential measurements. The as-synthetized zeolites presented negative zeta potentials, while APTMS functionalized zeolites showed slight positive potentials, and importantly, the cross-linked materials showed potentials that were substantially more positive. The GCE/BEA/APTMS/GO/NF did not show much improvement on BPE oxidation; however, the GCE/BEA/APTMS/GA/GO/NF electrode exceeded expectations. Thus, it suggests that the zeolite electrostatic surface features play a determinate role on analyte determination, and this could not be achieved by solely functionalizing GO. It appears that a more positively charged zeolite surface results in more favorable electrode interaction with analyte. A balance between GO and nanozeolite specific electrostatic features is necessary, and only achieved after using the GA based material, with surfaces more positively charged.

Additionally, the modified electrode did not show any fouling caused by the deposition of BPE oxidation products; phenomena that is commonly reported in bare or modified electrodes for the analysis of BPs [, , , , , , 15, 19, 22, 27, 28, 30, 31], resulting from the deposition of oxidation products hindering further analyte oxidation. This is usually an effect observed after multiple voltammetry cycles, and it was not observed for the number of cycles performed at the same electrode in this study.

Electrochemical behaviors of BPE at GCE/BEA/APTMS/GA/GO/NF with different scan rates (ν) were further investigated. Figure 3A shows the CV curves obtained. Figure 3B shows that the oxidation peak current increased linearly with scan rate in the range from 10 to 1000 mVs^{-1}, indicating that the oxidation of BPE at GCE/BEA/APTMS/GA/GO/
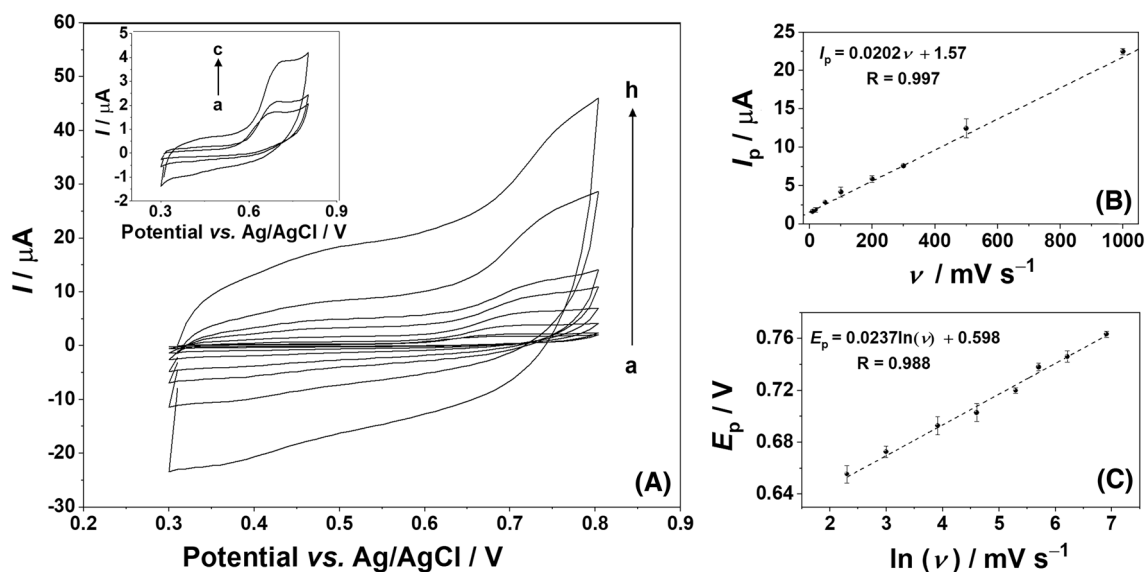
Fig. 3 A Cyclic voltammograms of 50 μM BPE at GCE/BEA/APTMS/GA/GO/NF with different scan rates. Curves (a–h) are obtained at 10, 20, 50, 100, 200, 300, 500, and 1000 mVs^{-1}, respectively. Inset: Curves a–c. **B** Dependence of the oxidation peak current (I_p) on the scan rate. **C** Dependence of the oxidation peak current potential (E_p) on the natural logarithm of scan rate (ν)

NF electrode was an adsorption-controlled process [58]. The regression equation were expressed as $I_p = (0.0202 \pm 0.0003)\nu + (1.57 \pm 0.06)$ (µA, mVs^{-1}, R = 0.997).

Figure 3C shows the relationship between the peak potential (E_p) and the natural logarithm of scan rate ν. It can be observed that the anodic peak potential E_p changed linearly versus $\ln(\nu)$ with a linear regression equation of $E_p = (0.024 \pm 0.001)\ln(\nu) + (0.598 \pm 0.006)$ (V, mVs^{-1}, R = 0.988) in the range of 10 to 1000 mVs^{-1}. For a totally irreversible electrode process, the relationship between the potential (E_p) and scan rate (ν) is expressed as reported by Laviron [58]:

$$E_p = E_0 + (RT/\alpha nF)\ln\left(RTk_s/\alpha nF\right) + (RT/\alpha nF)\ln(\nu)$$

Where α is transfer coefficient, k_s is standard rate constant of the reaction, n is the electron transfer number, ν is the scan rate, E_0 is the formal redox potential, R is the gas constant, T is the absolute temperature, and F is the Faraday constant ($T = 294$ K, $R = 8.314$ JK^{-1} mol^{-1}, and $F = 96,485$ Cmol^{-1}). According to the slope of the plot of E_p versus $\ln(\nu)$, the value of αn was calculated to be 1.05. Generally, α is assumed to be 0.50 in a totally irreversible electrode process. This allowed the inference that the electron transfer number (n) for oxidation of bisphenol E was around 2.

## 3.2 pH dependence of BPE at GCE/GO/BEA/APTMS/GA/NF

The effect of pH on the electrochemical responses of BPE at GCE/GO/BEA/APTMS/GA/NF was studied over the pH range of 2.0–9.0 using Britton–Robinson buffer (Fig. 4A). As the process was adsorption-controlled, 90 s magnetic stirring was employed before measurements to guarantee diffusion to the electrode surface and reproducible amounts of BPE at the electrode surface for the voltammetric cycles. The oxidation currents were very similar at pH values 2.0, 3.0, 5.0, and 7.0, slightly lower for pH 6.0 and considerable lower for pH values 4.0, 8.0, and 9.0. The pKa of BPE lies in the basic range (9.81–10.42 [59]), however, our observations do not follow any trend. This behavior was different to that reported for BPA [24], where a maximum was observed at pH 8.0 using a GCE electrode decorated with magnetic nanoparticles and reduced graphene oxide. As no similar studies to the best of our knowledge have been reported for BPE, we measured the behavior of BPA at the GCE/GO/BEA/APTMS/GA/NF electrode for comparison. Interestingly, results diverge from the reported [24], with a maximum at pH 2.0, moderate oxidation current reduction at pH 3.0, and slightly lower current (compared with pH 3.0) for the pH values from 4.0 to 9.0 (Fig. S4 for BPA CV curves). This indicated the influence of the electrode composition on the pH dependence. Clearly, though, the bisphenol structure influenced the interaction with the electrode, as BPE and
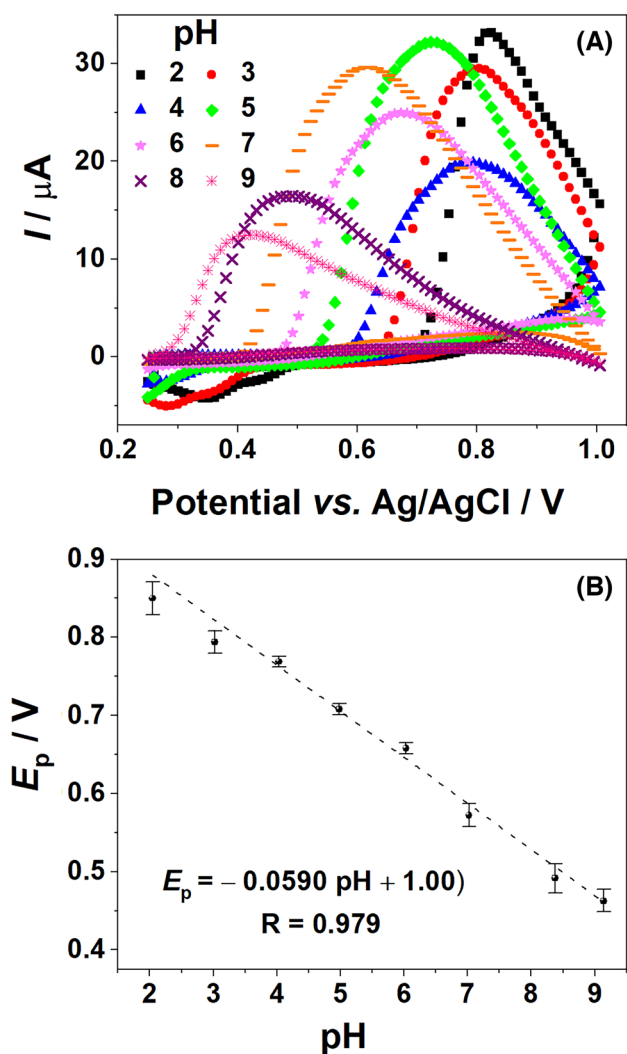
Fig. 4 **A** The CV curves of 50 µM BPE in different pH values (Britton–Robinson buffer) at GCE/GO/BEA/APTMS/GA/NF electrode. Background was first recorded in the absence of analyte and subtracted from the respective voltammograms. Scan rate 100 mVs^{-1}, N$_2$ atmosphere. **B** Dependence of the pH on the oxidation peak current potential (E_p)

BPA behaved differently at the GCE/GO/BEA/APTMS/GA/NF electrode. Based on the low variation in peak current intensity at pH 5 and 2 for BPE, we reasoned to use pH 5 for the continuation of the studies, and used phosphate buffer solution as carried out through the modification screening.

Further, the peak potential shifted negatively with the increase of pH value. The relationship between E_p and pH is shown in Fig. 4B for BPE, and obeys the equation $E_p = (-0.0590 \pm 0.003)\text{pH} + (1.00 \pm 0.02)$ (V, R = 0.979). A slope of about -59.0 mV per pH unit was close to the theoretical value of -57.6 mV/pH. This indicated that an equal number of electrons and protons were involved in this electrochemical reaction [, , , , 18, 24, 27–29], therefore, the electrooxidation of BPE at GCE/GO/BEA/APTMS/GA/NF
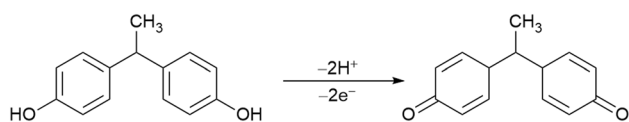
Fig. 5 Proposed electrochemical reaction of BPE

was a two-electron and two-proton process, as the number of electrons were estimated to be two in the previous section. The proposed electrochemical reaction equation of BPE is shown in Fig. 5.

3.3 Insights of the electrode surface

Figure S5 shows the SEM images of the bare GCE electrode (Fig. S5A) in comparison with the modified electrode before (GCE/GO/BEA/APTMS/GA) (Fig. S5B) and after NF coating (Fig. S5C). A flat surface was observed for the bare GCE, while agglomerates were evident at the modified electrode. The aggregates are caused by the interaction of the modifier components, BEA/APTMS/GA and GO, and may give rise to the synergistic effect discussed before, where the disposition of the modifiers benefits the electrostatic adsorption of BPE and the electron transfer, including an increase of the electrode surface area. Thorough characterization of BEA and BEA functionalized derivatives were previously reported [32], however, as the materials used in this work consisted of new batches, XRD, SEM, and FT-IR characterization data is presented in the Supplementary Information (Fig. S1), which are consistent with the previously reported data. FT-IR data (Fig. S2) provided evidence for the effective functionalization of GO. Bands at wavelengths between 1000 and 1200 cm^{-1}, were assigned to the $C-N$, $Si-O-Si$, and $Si-O-C$ bonds of the aminopropyl groups, as well as the $N-H$ broad band at aproximately 3200 cm^{-1} [52]. Furthermore, bands in the region 1350–1750 cm^{-1} were assigned to the bending mode of $CH-R-CH_3$ and methyl group $-CH_3$ of glutaraldehyde, as well as the $C=O$ stretching mode [, 32, 52].

3.4 Differential pulse voltammetric determination

Differential pulse voltammetry (DPV) was chosen to check the analytical performance of the electrode toward BPE. A non-systematic optimization was performed to check the influence of parameters such as accumulation time and potential. Potentials from 0 to 0.5 V where checked at a fixed time (60 s) with magnetic stirring, and no significant peak current increase was observed. However, the current depended on accumulation time. An interval from 0 to 180 s was tested, and an increase was observed for the first 90 s and no increase was observed over longer periods. Based on these tests, an accumulation potential of 0.5 V was applied

for 90 s for the DPV measurements. The DPV parameters were also tested for optimization, and the highest current was measured when increment potential, pulse period, pulse amplitude, and pulse width were adjusted to 0.075 mV, 0.4 s, 0.05 V, and 0.075 s, respectively. Under the optimized conditions, DPV of a series of BPE concentrations were collected, as shown in Fig. 6A. A linear relationship between oxidation current (I_p) and BPE concentration (C_{BPE}) was obtained over the range of 0.07 and 4.81 µM (Fig. 6B), and the regression equation was expressed as $I_p = (0.52 \pm 0.01) C_{BPE} + (0.011 \pm 0.001)$ (µA, µM) with a correlation coefficient of 0.995. The limit of detection (LOD) was estimated to be 0.056 µM (S/N = 3). For means of comparison, BPA was also tested and a linear regression was obtained for a linear range of 0.2–4.00 µM, which obeyed the equation $I_p = (1.00 \pm 0.04) C_{BPA} + (0.170 \pm 0.007)$ (µA, µM, R = 0.991)) and LOD = 0.19 µM (S/N = 3) (See Fig. S6 for DPV curves and linear regression fitting). The optimized conditions for the two bisphenols were the same indicating that the electrode was not selective toward bisphenols of similar structure; although a lower LOD was obtained for BPE. In the work reported by Lu et al. using a MOF/tyrosinase biosensor (2016) [45], the LOD for BPE was 0.015 µM, in a linear range of 0.05–3.0 µM, which is of similar sensitivity to the electrode in this work. The observed differences regarding BPE and BPA electrode sensitivity and behavior was also in line with previous observations of the substituent group properties (electron acceptor or electron donor) on the bisphenol framework having strong influence on the electrode performance. Although the electrochemical determination of BPE is not vastly reported, the analytical performance of the presented sensor was comparable to other graphene oxide or zeolite material-based sensors reported in the literature for the determination of BPA, what is pertinent considering that both BP's have shown similar behavior in this work. Linear ranges and LOD are summarized in Table 1. It can be seen that the presented sensor displays a comparable linear range with an acceptable detection limit.

3.5 Interference, repeatability, and stability

In order to check the robustness of the methodology, an interference assay was performed using 4-chlorophenol (CP), BPA, BPF, TBrBPA, and duroquinone (DQ). For this, the I_p of 2 µM BPE was compared with the I_p of 2 µM BPE in solutions containing the same concentration of the possible interfering chemical. Figure 7A presents the relative I_p percentage recovery of the isolated BPE (100%) within the mixtures. Among the tested compounds, only BPA showed a substantial interference of around 40%. Nevertheless, it can be pointed out that a 100% interference would be expected if BPE and BPA had no specific interactions each with the electrode surface as they oxidize at the same voltage (within
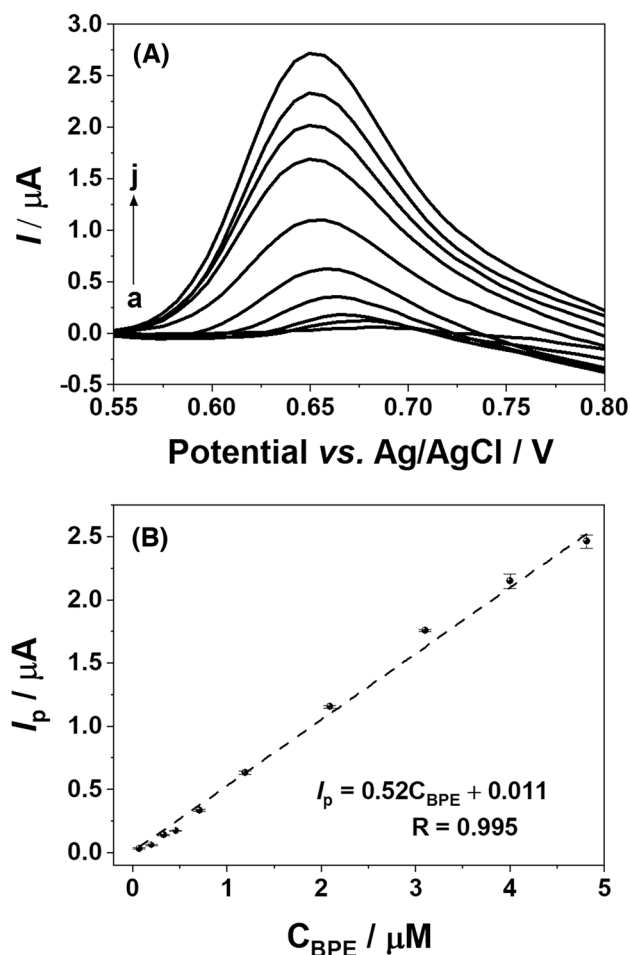
Fig. 6 **A** The DPV curves for different BPE concentration (C_{BPE}): a −0.07, b −0.20, c −0.33, d −0.46, e −0.71, f −1.19, g −2.09, h −3.10, I −4.00, and j −4.81 μM. **B** Linear regression for the calibration C_{BPE} versus anodic peak current (I_p). The increment potential, pulse period, pulse amplitude, and pulse width were adjusted at 0.075 mV, 0.4 s, 0.05 V, and 0.075 s, respectively

error). The analytical equations obtained (DPV calibration of BPE and BPA, Fig. 6B and Figure S6B, respectively) showed different slopes, 0.52 ± 0.01 (BPE) and 1.00 ± 0.04 (BPA), which numerically showed differences in the rate current/concentration that can be attributed to the interaction between analyte and electrode.

To verify electrode repeatability and stability, two different GCE electrodes were coated on same day under the same conditions, and used to measure 2 μM BPE solutions on the day of preparation, and after 3 and 7 days, Fig. 7B. Repeatability was analyzed considering the percentage difference between consecutive measurements on the same day for one electrode, which were found to be lower than 3%. Good stability was also verified, as the electrodes did not significantly present higher or lower current output in the seven-day time interval tested, with lower and maximum relative I_p within all measurements showing less than 10% difference. It is fair to point out that after measurements the electrodes were simply rinsed with distilled water, dried with a nitrogen flush and stored at room temperature in a closed container.
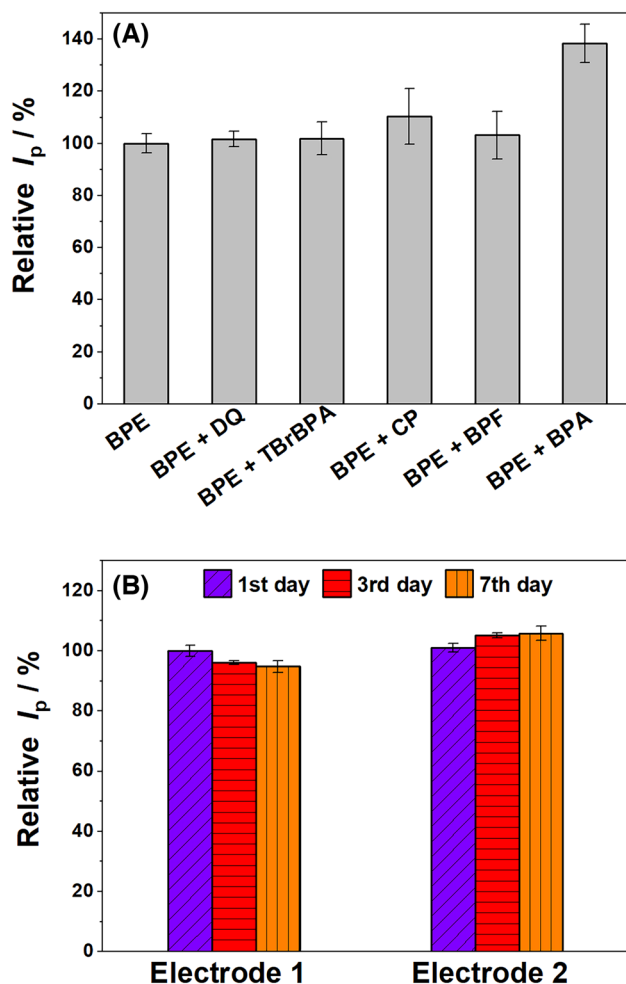
3.6 Application to analysis

To validate the method proposed, the standard addition method was employed, and recoveries ranging from 91 to 109% were obtained, with residual standard deviation up to 6%, Table 2. The recovery tests indicate that the proposed method is suitable for BPE determination.

4 Conclusion

In summary, it has been demonstrated that the modification of GCE with BEA/APTMS/GA/GO/NF nanocomposite was effective for the highly sensitive determination of BPE. The

Table 1 Comparison of the analytical performance of this work electrode with other electrochemical sensors graphene oxide/nanozeolite based for the determination of BPE and BPA

Sensor	Bisphenol	Linear range/μM	Detection limit/μM	Refs
GO-poly(NPBimBr)/GCE	BPA	0.2–10.0	0.017	[20]
SiO$_2$/GO/AgNP/GCE	BPA	0.1–2.6	0.127	[21]
GO/APTES–MIP/GCE	BPA	0.006–0.1 and 0.2–20	0.003	[22]
RGO/M-GCE	BPA	0.01–200	0.004	[26]
ZnTsPc/f-GN/GCE	BPA	0.05–4.0	0.02	[23]
ZrO$_2$(20%)/Nano-ZSM-5/GCE	BPA	0.006–600.0	0.003	[44]
PDMS@SNCM/ITO	BPA	1–100	0.23	[31]
α-MoO$_3$/CPE	BPA	0.03–1.6	0.015	[30]
CuMOFs-Tyr-Chi/GCE	BPE	0.05–3.0	0.015	[45]
	BPA	0.05–3.0	0.013	
ITO modified with A-G-GO	BPA	5–1000	5	[46]
	BPE	10–1000	10	
GCE/BEA/APTMS/GA/NF	BPE	0.07–4.8	0.056	This work
	BPA	0.2–4.0	0.19	

Fig. 7 A Interference test for BPE determination in the presence of BPA, BPF, TBrBPA, DQ, and CP. DPV measurements under the optimized conditions were employed to detect 2 μM of BPE only, or the same amount of BPE in the presence of 2 μM of the tested interfering compound. Relative anodic current (I_p) was calculated considering the assay with no interfering as 100%. **B** Repeatability and stability tests for BPE determination using two different electrodes. Measurements performed at the day of preparation, after 3 days, and after 7 days, using 2 μM BPE solutions. Relative anodic current (I_p) was calculated considering Electrode 1 first day as 100%

Table 2 Tap water analysis and recovery tests of BPE oxidation at GCE/GO/BEA/APTMS/GA/NF electrode

Samples	C_{BPE} added/μM	C_{BPE} found/μM	RSD/%	Recovery/%
Tap water	0	0	–	–
	0.483	0.530	1.46	91.12
	1.049	1.050	2.82	99.99
	1.557	1.570	3.63	99.14
	2.026	2.080	2.31	97.41

interference toward CP, DQ, BPF and TBrBPA. Despite BPE and BPA having very similar peak potential dependence of pH, the current response diverged, which was in agreement with the observation of a higher response for BPE determination compared to BPA using the optimized analytical method proposed. These differences can be hypothesized as response to BPs structural differences, what leads to specific interactions between analytes and electrode surface and may be influenced by the observed surface agglomerates. The results suggest that the functionalized nanozeolite/graphene-based electrode is a potential platform for bisphenols determination.

Declarations

modifier composition, showed a synergistic effect toward electrode current response compared to bare GCE. This is hypothesized to be related to electrostatic changes on the zeolite surface due to the functionalization using APTMS and GA, favoring analyte adsorption, as the electrochemical process was adsorption-controlled and involves an equal number of electrons and protons. The analytical method proposed presented good detection limits and linear range, which are very close to the limit and range for the only electrochemical sensor for BPE reported (CuMOFs-Tyr-Chi/GCE) [45]. In addition, the electrode has shown good reproducibility, repeatability and storage stability, as well as low

References

1. Sinha A, Wu L, Lu X, Chen J, Jain R (2018) Anal Chim Acta 998:1
2. Wang G, Wu F, Zhang X, Luo M, Deng N (2006) J Hazard Mater 133:85
3. Rosenmai AK, Dybdahl M, Pedersen M, Alice van Vugt-Lussenburg BM, Wedebye EB, Taxvig C, Vinggaard AM (2014) Toxicol Sci 139:35
4. Shi M, Whorton AE, Sekulovski N, MacLean JA, Hayashi K (2019) Toxicol Sci 172:303
5. Pelch K, Wignall JA, Alexandra E. Goldstone, Pam K. Ross, Robyn B. Blain, Andrew J. Shapiro, Stephanie D. Holmgren, Hsieh J-H, Svoboda D, Auerbach SS, Parham FM, Masten SA, Walker V, Rooney A, Thayer KA (2019) Toxicol 424:152235
6. Chen MY, Ike M, Fujita M (2002) Environ Toxicol 17:80
7. Ragavan K, Rastogi NK, Thakur M (2013) TrAC, Trends Anal Chem 52:248
8. Wang X, Lu X, Chen J (2014) Trends Environ Anal Chem 2:25
9. Portaccio M, Di Tuoro D, Arduini F, Moscone D, Cammarota M, Mita DG, Lepore M (2013) Electrochim Acta 109:340
10. Xu G et al (2013) Anal Methods 5:3328
11. Kunene K, Sabela M, Kanchi S, Bisetty K (2020) Waste Biomass Valorization 11:1085
12. Yang J, Wang X, Zhang D, Wang L, Li Q, Zhang L (2014) Talanta 130:207
13. Wang X, Yang L, Jin X, Zhang L (2014) Food Chem 157:464
14. Goulart LA, Gonçalves R, Correa AA, Pereira EC, Mascaro LH (2018) Microchim Acta 185:12
15. Sidwaba U, Ntshongontshi N, Feleni U, Wilson L, Waryo T, Iwuoha EI (2019) Electrocatalysis 10:323
16. Shim K, Kim J, Shahabuddin M, Yamauchi Y, Hossain MSA, Kim JH (2018) Sens Actuators, B Chem 255:2800
17. Wang Y, Chen F, Ye X, Wu T, Wu K, Li C (2017) Sens Actuators, B Chem 245:205
18. Gan T, Shi Z, Wang K, Chen Y, Sun J, Liu Y (2015) J Solid State Electrochem 19:2299
19. Güney S, Güney O (2017) Electroanalysis 29:2579
20. Wang Y, Li C, Wu T, Ye X (2018) Carbon 129:21
21. Campos AM, Raymundo-Pereira PA, Cincotto FH, Canevari TC, Machado SAS (2016) J Solid State Electrochem 20:2503
22. Dadkhah S, Ziaei E, Mehdinia A, Kayyal TB, Jabbari A (2016) Microchim Acta 183:1933
23. Hou K, Huang L, Qi Y, Huang C, Pan H, Du M (2015) Mater Sci Eng, C 49:640
24. Zhang Y, Cheng Y, Zhou Y, Li B, Gu W, Shi X, Xian Y (2013) Talanta 107:211
25. Hu Y, Wang S, Guo Z, Hu Y, Xie H (2018) ChemElectroChem 5:2449
26. Shen R, Zhang W, Yuan Y, He G, Chen H (2015) J Appl Electrochem 45:343
27. Yin H, Zhou Y, Cui L, Liu X, Ai S, Zhu L (2011) J Solid State Electrochem 15:167
28. Zhao J, Ma Y, Hou X, Li L, Zheng P, Li C (2015) J Solid State Electrochem 19:1571
29. Yin H, Zhou Y, Ai S, Chen Q, Zhu X, Liu X, Zhu L (2010) J Hazard Mater 174:236
30. Antoniazzi C, de Lima CA, Marangoni R, de Castro EG, Santana ER, Spinelli A (2020) Microchem J 159:105528
31. Wang J, Yu J, Yu Y, Luo Z, Li G, Lin X (2023) Food Chem 405:134806
32. de Vasconcellos A, Miller AH, Aranda DAG, Nery JG (2018) Colloids Surf, B 165:150
33. Salih FE, Achiou B, Ouammou M, Bennazha J, Ouarzane A, Younssi SA, El Rhazi M (2017) J Adv Res 8:669
34. Maicaneanu A, Varodi C, Bedelean H, Gligor D (2014) Chem Erde-Geochem 74:653
35. Zhang R, Ma J, Wang W, Wang B, Li R (2010) J Electroanal Chem 643:31
36. He P, Wang W, Du L, Dong F, Deng Y, Zhang T (2012) Anal Chim Acta 739:25
37. Carvalho R, Lemos F, Lemos M, Cabral J, Ribeiro FR (2007) J Mol Catal A: Chem 278:47
38. Dong J, Zhou X, Zhao H, Xu J, Sun Y (2011) Microchim Acta 174:281
39. Zhou X, Yu T, Zhang Y, Kong J, Tang Y, Marty J-L, Liu B (2007) Electrochem Commun 9:1525
40. Celikbicak O, Bayramoglu G, Yılmaz M, Ersoy G, Bicak N, Salih B, Arica MY (2014) Microporous Mesoporous Mater 199:57
41. Kirdeciler SK, Soy E, Öztürk S, Kucherenko I, Soldatkin O, Dzyadevych S, Akata B (2011) Talanta 85:1435
42. Noroozifar M, Khorasani-Motlagh M, Akbari R, Parizi MB (2011) Biosens Bioelectron 28:56
43. Yu T, Zhang Y, You C, Zhuang J, Wang B, Liu B, Kang Y, Tang Y (2006) Chem A Eur J 12:1137
44. Kaur B, Satpati B, Srivastava R (2016) RSC Adv 6:65736
45. Lu X, Wang X, Wu L, Wu L, Fu L, Gao Y, Chen J (2016) ACS Appl Mater Interfaces 8:16533
46. Vaghela C, Kulkarni M, Karve M, Zinjarde S (2022) J Environ Chem Eng 10:107360
47. Liu E, Zhang X (2014) Anal Methods 6:8604
48. Gan T, Wang Z, Gao J, Sun J, Wu K, Wang H, Liu Y (2019) Sens Actuators, B Chem 282:549
49. Manea F, Ihos M, Remes A, Burtica G, Schoonman J (2010) Electroanalysis 22:2058
50. Narang J, Malhotra N, Singhal C, Mathur A, Chakraborty D, Anil A, Ingle A, Pundir CS (2017) Biosens Bioelectron 88:249
51. Larlus O, Mintova S, Wilson ST, Willis RR, Abrevaya H, Bein T (2011) Microporous Mesoporous Mater 142:17
52. Lin Y, Jin J, Song M (2011) J Mater Chem 21:3455
53. Mazzotta E, Malitesta C, Margapoti E (2013) Anal Bioanal Chem 405:3587
54. Yu C, Gou L, Zhou X, Bao N, Gu H (2011) Electrochim Acta 56:9056
55. Zhao Q, Wu W, Wei X, Jiang S, Zhou T, Li Q, Lu Q (2017) Sens Actuators, B Chem 248:673
56. Zhao Q, Zhang K, Yu G, Wu W, Wei X, Lu Q (2016) Talanta 151:209
57. Erogul S, Bas SZ, Ozmen M, Yildiz S (2015) Electrochim Acta 186:302
58. Laviron E (1974) J Electroanal Chem Interfacial Electrochem 52:355
59. Regueiro J, Breidbach A, Wenzl T (2015) Rapid Commun Mass Spectrom 29:1473

Authors and Affiliations

Alex H. Miller[1,2,3] · **Huong Thi-Thanh Nguyen**[1] · **José G. Nery**[2] · **Alistair J. Fielding**[1]

1 Centre for Natural Products Discovery, School of Pharmacy and Biomolecular Science, Liverpool John Moores University, James Parsons Building, Byrom Street, Liverpool L3 3AF, UK

2 Physics Department, Institute of Biosciences, Letters, and Exact Sciences—IBILCE/São Paulo State University—UNESP, São José Do Rio Preto, São Paulo 15054-000, Brazil

3 Present Address: Department of Chemistry, University of York, Heslington, York YO10 5DD, UK